Chain Photoreduction of CCl_3F in TiO_2 Suspensions: Enhancement Induced by O_2

Kurt Winkelmann,*,† Robert L. Calhoun,‡ and German Mills*,‡

Department of Chemistry, Florida Institute of Technology, Melbourne, Florida 32901, and Department of Chemistry, Auburn University, Auburn, Alabama 36849

Received: July 31, 2006; In Final Form: October 18, 2006

Trichlorofluoromethane (CFC 11) was photoreduced in aqueous suspensions of TiO_2 particles containing HCO_2^- ions and air. Dissolved O_2 inhibited the reaction during an induction period that preceded the rapid formation of chloride ions. Reaction rates were higher in systems containing O_2 as compared to analogous reactions that occurred in anaerobic suspensions. High photonic efficiencies of Cl^- formation (≥ 15) were achieved using suspensions with pH $\geq$ 5. As was the case for studies with air-free suspensions, reactions are best described using a photoinitiated chain mechanism that produced $CHCl_2F$ and Cl^- during the propagation steps. The enhanced yields obtained in the presence of air are attributed to the removal by O_2 of electrons trapped in the oxide, which are converted first into H_2O_2 and then into reducing radicals that participate in the chain process. Enhanced yields of Freon photoreduction were also observed during illumination of air-free suspensions containing hydrogen peroxide, which were interpreted using a similar mechanism.

Introduction

Photolysis of semiconductor particles dispersed in liquids is a simple way to initiate chemical reactions of inorganic and organic chemicals dissolved in the fluid phase.[1−3] Exposure of particulate semiconductors to light results in formation of charge carriers consisting of conduction band electrons (e_{cb}^-) and valence band holes (h_{vb}^+) able to induce redox transformations. A popular research area involving semiconductor photochemistry employs aqueous suspensions of TiO_2 powder to achieve oxidative dehalogenations of organic compounds that pollute the terrestrial and atmospheric environments.[2,3] Generation of charge carriers in TiO_2 is followed by formation of free radicals on or next to the oxide surface.[4] The oxidative decay of the pollutants is a consequence of their reactions with the photogenerated radicals. A general limitation of photoprocesses based on semiconductor particles is that the light-produced free radicals usually participate in side reactions, which limit the efficiency of the desirable transformations. Exceptions are cases in which the free radicals have been employed to initiate chain reactions.[5]

Another obvious drawback of semiconductor-induced oxidations is that such reactions are ineffectual for fully halogenated compounds because the C atoms present in such compounds are already in their highest oxidation state. However, earlier radiation chemical investigations have demonstrated that chain reductive dehalogenations occur when fully halogenated hydrocarbons react with strongly reducing radicals.[6] Recent studies have shown that a similar strategy can be employed to achieve efficient reductive dehalogenations of chlorofluorocarbons (CFCs) via illumination of TiO_2 suspensions. The CFCs are a very important class of pollutants banned by the Montreal Protocol, of which CCl_3F has made the largest contribution to the stratospheric ozone depletion.[7] Illumination of air-free TiO_2 suspensions containing formate ions and CCl_3F resulted in the reduction of the halocarbon through a free-radical chain mechanism with $CHCl_2F$ as the only halogenated product and quantum efficiencies larger than 5.[8] This method of selective dehalogenations of CFCs through chain photoreactions initiated by TiO_2 particles was originally demonstrated using CCl_2FCF_2Cl and CCl_3CF_3 (CFC 113 and CFC 113a).[9] CCl_4 also undergoes fast dechlorination upon illumination of TiO_2 suspensions at high pH through processes believed to involve chain reactions.[10]

The presence of high HCO_2^- concentrations enabled these ions to react fast with valence band holes or with $OH^\bullet$ radicals formed during oxidation of H_2O, interfering with the recombination of e_{cb}^- with $h_{vb}^+/OH^\bullet$.[11] Formate ions were employed as scavengers of $h_{vb}^+/OH^\bullet$ because the reaction of HCO_2^- with these oxidizers yields $^\bullet CO_2^-$ radicals.[12] These species are strongly reducing radicals,[13] able to induce reductive dehalogenations of CFCs.[14] Reduction of chlorofluorocarbons can form their hydrogen-substituted analogues (HCFCs), which currently serve as replacements for CFCs in many industrial processes.[15] Development of an efficient and cost-effective method for the conversion of CFCs to HCFCs could speed the process of replacing chlorofluorocarbons that have yet to be destroyed or that are being recycled and reused. This would decrease the overall amount of CFCs being accidentally released into the atmosphere through spills and leaks.

Data are presented here showing that the CCl_3F reduction induced by photolysis of TiO_2 suspensions is enhanced in an oxygenated environment. Interference by oxygen molecules is a characteristic of chain reactions involving reducing free radicals,[16] but in certain systems O_2 has been found to enhance the rate of these processes.[10a,17] Oxygen is frequently used as a scavenger of e_{cb}^- from the TiO_2 surface to diminish charge carrier recombination and to promote oxidations involving $h_{vb}^+/OH^\bullet$.[2,3] In addition, oxidation of $^\bullet CO_2^-$ by O_2 in solution is diffusion-controlled.[18] Given that the reduction of CCl_3F is initiated by $^\bullet CO_2^-$ and by e_{cb}^- in oxygen-free suspensions,[8] inhibition of the chain reaction by O_2 was expected. However, efficiencies of CCl_3F reduction greater than those observed in air-free systems were measured after an induction period in irradiated TiO_2 suspensions containing O_2. Additional reaction

* Authors to whom correspondence should be addressed. E-mail: kwinkel@fit.edu (K.W.); millsge@auburn.edu (G.M.).
† Florida Institute of Technology.
‡ Auburn University.

10.1021/jp0648893 CCC: $33.50
Published on Web 12/07/2006

steps are proposed to explain the faster reaction rate caused by dissolved oxygen.

Experimental Methods

Unless otherwise noted, all chemicals were reagent grade and were used as received from Fisher or Aldrich. Aqueous solutions contained water that was deionized by a Milli-Q-Plus system (Millipore, $\rho \geq 18.2$ MΩ). Occasionally, results were verified using HPLC grade water. Aqueous suspensions contained TiO_2 particles (Degussa P-25, 30-nm average diameter) in 110.0 mL of formic acid/sodium formate buffer. Throughout this study, the buffer concentration is given in terms of $[HCO_2^-] + [HCO_2H]$. Several blank experiments were performed using silicon dioxide powder (Degussa Aerosil 380, 7-nm average particle diameter) instead of TiO_2. Suspensions containing H_2O_2 were prepared using a fresh, stabilizer-free, 30% (v/v) H_2O_2 stock solution. Air-free systems were prepared by bubbling the buffered TiO_2 suspension with Ar for 30 min under continuous stirring within a photochemical reactor vessel sealed with rubber septa. Liquid CCl_3F was degassed via three freeze−pump−thaw cycles prior to injection into the sealed photoreactor using a gastight syringe. Suspensions were purged with Ar prior to addition of CCl_3F to avoid excessive vaporization of the CFC (bp = 23.7 °C). For experiments with systems that were initially air-saturated, neither the aqueous TiO_2 suspension nor the CFC liquid was degassed, but the illuminations were performed after sealing the photoreactor. All suspensions contained two liquid phases because of the low solubility of CCl_3F in water (8.1×10^{-3} M or 82 μL in a 110.0 mL suspension).[19] Stirring created numerous small droplets of CFC liquid distributed throughout the aqueous phase.

To determine the effects of O_2 during the photochemical reaction, known volumes of oxygen gas (99.99% purity) were injected into suspensions degassed with Ar. This procedure yielded suspensions containing O_2 equilibrated between the suspension and the 60 mL of photoreactor headspace. Since the solubility of oxygen in a formic acid/formate buffer solution is not known, the amount of O_2 in the system is expressed here as the moles of gas added to the photoreactor. For air-saturated buffer solutions the amount of O_2 in the photoreactor was estimated to be between $5.2-5.5 \times 10^{-4}$ mol. The upper limit corresponds to the amount of oxygen from air (21% by volume) present in the headspace plus the number of moles of gas that would dissolve in 110.0 mL of pure water.[20] However, as is typical for electrolyte solutions,[20] $[O_2]$ decreases when the ionic strength increases. The lower limit results from assuming that the headspace contained most of the oxygen molecules, with a negligible amount of O_2 dissolved in the buffer. This calculation treated O_2 as an ideal gas at 23 °C. Because of the small CCl_3F volume used in these experiments, the amount of O_2 dissolved in the CFC liquid was not significant for this calculation.

Experimental procedures and equipment utilized in this study have been described elsewhere.[8,9] Briefly, a double-walled borosilicate glass vessel with an internal volume of 170 mL was employed as a photoreactor. *Caution should be taken when performing similar experiments because sealed photoreactors shattered on several occasions due to a buildup of pressure within the vessel during irradiation.* After degassing (if needed), the mixtures were stirred for at least 15 min at 320 rpm using a Thermix 120 MR magnetic stirring plate prior to illumination. The resulting kinetic data were independent of the length of this equilibration period beyond 15 min. Concentrations of Cl^- and F^- were determined in situ using ion selective electrodes (ISE) under continuous irradiation and stirring. The ISE were calibrated in the dark prior to each experiment under conditions duplicating those of the photolysis experiments. Because only one electrode could be used during a given experiment, chloride and fluoride concentrations were determined via separate kinetic runs. Most experiments were performed at least twice; deviations of up to 30% were noted periodically.

Light from a PTI 1010 S system with a 150 W Xe arc lamp was filtered using a 10-cm water filter and an IR absorbing filter to remove infrared radiation. Photons with wavelengths between 320 and 385 nm (maximum transmittance at 360 nm) were selected by a Kopp GS-7-60 filter and were focused on the flat, lateral window (38 mm × 51 mm) of the photoreactor. Variations in light intensity (I_o) were accomplished by inserting neutral density filters into the light path. Aberchrome 540 actinometry was used to measure I_o for each irradiation.[21] The effectiveness of the photoreduction is expressed as the photonic efficiency (P.E.), which corresponds to the reaction rate divided by the flux of incident photons.[2] Procedures that attempt to account for the scattering of light by the oxide particles have been suggested,[22] but none of these methods were used systematically since they are unable to correct the light-scattering effects induced by the Freon droplets. Given that I_o is always equal to or greater than the absorbed intensity, P.E. is a lower limit to the quantum yield of the photochemical reaction.

Previous investigations demonstrated that the maximum efficiency for a variety of photoreactions, including the reduction of Freons, is achieved using 0.50 g L^{-1} TiO_2.[3,9] Hence, unless otherwise stated, the suspensions contained 2.0 mL CCl_3F, 110.0 mL of 0.300 M sodium formate/formic acid buffer at pH 5.9 and 0.50 g L^{-1} TiO_2. Incident light intensities for typical reactions varied between $1.0-1.1 \times 10^{-6}$ M photons s^{-1}. Identification of gaseous products was performed using a Varian 3700 gas chromatograph (DB5 column from J & W Science) connected to a VG 7070E mass spectrometer. GC-MS analysis of products from the photoreaction was performed on a standard TiO_2 suspension containing CCl_3F photolyzed for 1 h using samples from the reactor headspace as well as from the aqueous and CFC liquid phases. Product identification was carried out by comparing their MS spectra with those of known halogenated compounds.

Results

As in the case of air-free systems,[8] chloride and fluoride ions were generated when air-saturated, aqueous suspensions containing TiO_2, formate ions, and CCl_3F were exposed to light. Negligible amounts of products were detected upon photolysis of solutions free of TiO_2. Irradiation of suspensions containing equivalent amounts of SiO_2 powder (on the basis of total particle surface area or mass) produced less than 2% of the $[Cl^-]$ measured in analogous TiO_2 suspensions. Visual analysis showed that no TiO_2 powder was present in the CFC liquid phase. No photoreaction was induced by ambient light and degassing suspensions with nitrogen or argon gas yielded identical kinetic results. Artificial photovoltages are induced during direct illumination of the ISE electrodes.[9] The high TiO_2 particle concentration present in the suspensions suppressed these artifacts since photolysis of CFC-free systems showed that the ISE photovoltage was <0.2% of the voltage change observed during the slowest stage (induction period) of the reaction. Although H^+ is produced as a byproduct of CFC photoreactions, no pH changes were detected because of the high concentration of formate buffer used in the suspensions.

Figure 1 depicts the growth of $[Cl^-]$ and $[F^-]$ as a function of photolysis time and demonstrates that both ions were formed

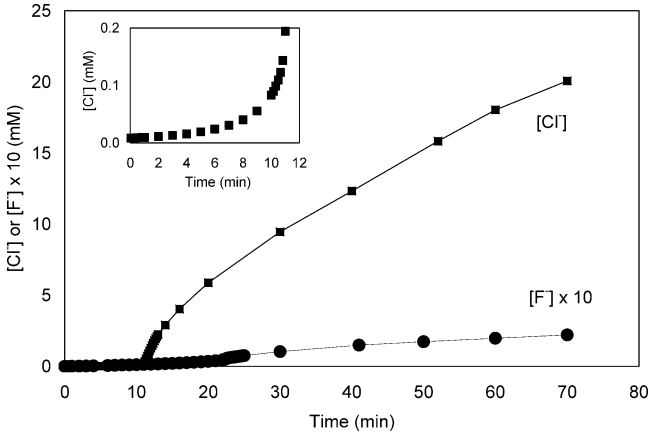

Figure 1. Plot of $[Cl^-]$ (■) and $[F^-]$ (× 10) (●) as a function of time for aerated suspensions containing 0.30 M formic acid/formate buffer, 2.0 mL CCl_3F, and 0.50 g L^{-1} TiO_2, irradiated with $I_o = 1.0 \times 10^{-6}$ M photons s^{-1} and pH = 5.9. Displayed in the inset is an expanded view of $[Cl^-]$ vs time during the induction period.

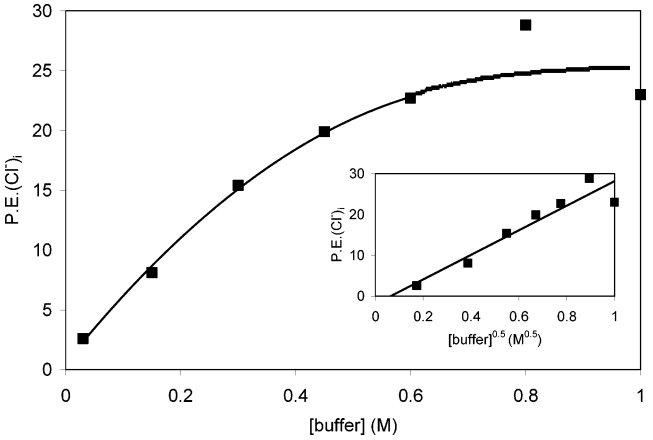

Figure 2. P.E.$(Cl^-)_i$ vs $[HCO_2^-]$. Suspensions were air-saturated, were irradiated with $I_o = 1.0 \times 10^{-6}$ M photons s^{-1}, and were buffered at pH 5.9 with 2.0 mL CCl_3F and 0.50 g L^{-1} TiO_2. The linear relationship between P.E.$(Cl^-)_i$ and $[HCO_2^-]^{0.5}$ is shown in the inset.

simultaneously upon irradiation of air-saturated, aqueous TiO_2 suspensions containing formate ions and CCl_3F. The transformation of CFC 11 was characterized by a slow initial reaction (the induction period); chloride ion concentrations obtained during this process are included in the inset. Efficient reduction of CFC 11 began only after completion of the initial step. The induction period typically lasted 10−20 min, although lengths as short as 8 min and as long as 25 min were occasionally noted. The duration of the induction period was hard to reproduce among duplicate measurements. The fact that $[Cl^-]$ and $[F^-]$ were determined in separate kinetic runs accounts for the different duration of the induction periods noticed in Figure 1. Factors that influenced the length of the induction period were the initial amount of O_2 present in the photoreactor and incident light intensity but other experimental parameters, such as buffer pH or buffer concentration, had no affect. Air-saturated suspensions exhibited a ratio of $r(Cl^-)/r(F^-)$ close to 3:1 during the first minute of illumination, where $r(Cl^-)$ and $r(F^-)$ are the rates at which chloride and fluoride are photogenerated. Such a ratio suggests that complete dehalogenation of CFC 11 took place according to

$$CCl_3F + 4e^- + 4H^+ + O_2 \rightarrow CO_2 + 3HCl + HF \quad (1)$$

Similar dehalogenations have been observed when halomethanes are reduced in aqueous air-saturated systems.[10b,23,24] The amounts of products ($[Cl^-] \leq 200\ \mu M$, $[F^-] \leq 50\ \mu M$) detected during the induction period were much smaller than those measured thereafter. Efforts to fit the kinetic data to any simple rate law were unsuccessful. For these reasons, analysis of the kinetic data focused on results obtained during the second stage of the CCl_3F transformation.

Reaction rates were highest at the beginning of the second process and remained constant for about 1 min before gradually decreasing. Data obtained during the early stage of the second process were used to calculate initial rates of chloride and fluoride formation, $r(Cl^-)_i$ and $r(F^-)_i$, and the corresponding photonic efficiencies, P.E.$(Cl^-)_i$ and P.E.$(F^-)_i$, respectively. These parameters were employed to characterize the kinetics of the photoreaction. The initial rates of chloride and fluoride formation were 700 and 100 times higher, respectively, as compared to the values measured at the start of the induction period. In all experiments involving suspensions prepared with oxygen, $r(Cl^-)_i$ was much higher than $r(F^-)_i$ during the second step. Efficiencies of P.E.$(Cl^-)_i = 16$ and P.E.$(F^-)_i = 0.29$ were obtained from the data of Figure 1. Throughout this phase of the reaction, Cl^- concentrations were approximately 75 times higher than $[F^-]$. The amount of chloride measured after 30 min of irradiation exceeded both the solubility limit of CCl_3F in H_2O (8.1 mM)[19] and the "concentration" of TiO_2 formula units (6.3 mM) in the suspension. GC-MS analysis of an aerated TiO_2 suspension containing 2 mL CCl_3F and 0.3 M HCO_2^-/HCO_2H buffer at pH 5.9 illuminated for 1 h yielded $CHCl_2F$ as the only gaseous halogenated product. Efforts to detect additional possible products, such as CH_2ClF, CCl_2F-CCl_2F, $CClF{=}CClF$, or other halogenated ethylenes, were not successful. Trace amounts of CCl_2F_2 (but not of $CHCl_2F$) were noticed occasionally, which is an impurity found in commercial samples of CFC 11.

Figure 2 illustrates the dependence of P.E.$(Cl^-)_i$ on formate buffer concentration. At pH = 5.9, formate accounted for 99.4% of the buffer, meaning that the [buffer] can be represented as $[HCO_2^-]$. The initial photonic efficiencies increased steadily with buffer concentration, and over 20 mM Cl^- was produced after 1 h of irradiating suspensions that contained more than 0.3 M buffer. Depicted in the inset of Figure 2 is the linear relationship between P.E.$(Cl^-)_i$ and $[HCO_2^-]^{0.5}$. P.E.$(Cl^-)_i$ approached zero in suspensions containing lower buffer concentrations, implying that the best-fit line in the inset was expected to intersect the origin as well. Linear regression analysis determined that the actual small intercept value (−1.9) was within one standard deviation of the anticipated value of zero. A straight line was also obtained when P.E.$(Cl^-)_i^{-1}$ was plotted as a function of $[HCO_2^-]^{-1}$, which in earlier studies of the phototransformations of halogenated compounds was interpreted as indicative of processes controlled by reactions on the TiO_2 surface.[25] This interpretation conflicts with a significant amount of evidence, such as the high P.E.$(Cl^-)_i$ values shown in Figures 2, 3, and 5, that the CFC photoreduction actually occurred through a chain reaction. Furthermore, earlier results involving CCl_3F reduction in degassed TiO_2 suspensions were also consistent with a chain mechanism.[8] Therefore, the present data was analyzed within the paradigm of a chain process as well.

As shown in Figure 3, the efficiency of Cl^- generation increases as the acidity decreases up to pH = 5 and remains fairly constant thereafter. Variations in pH were achieved by changing the ratio of $[NaHCO_2]$ to $[HCO_2H]$ while maintaining the total buffer concentration constant at 0.3 M. Between pH 3

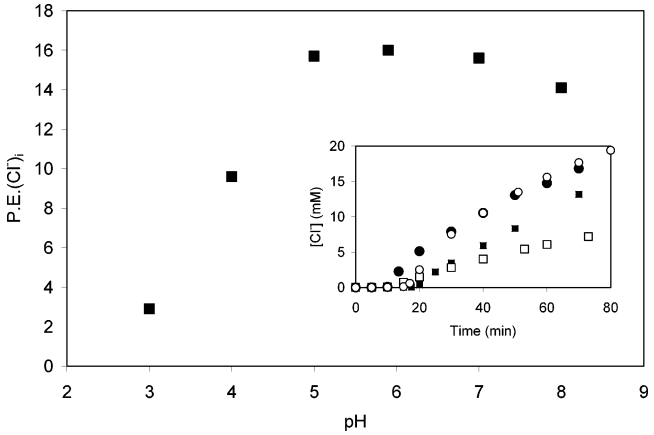

Figure 3. Effect of pH on P.E.$(Cl^-)_i$ of aerated suspensions containing 0.30 M formic acid/formate buffer, 2.0 mL CFC 11, and 0.50 g L^{-1} TiO_2. Suspensions were illuminated with $I_o = 1.0 \times 10^{-6}$ M photons s^{-1}. Presented in the inset is the evolution of Cl^- over time for suspensions at pH 3.0 (□), 4.0 (■), 5.9 (●), and 8.0 (○).

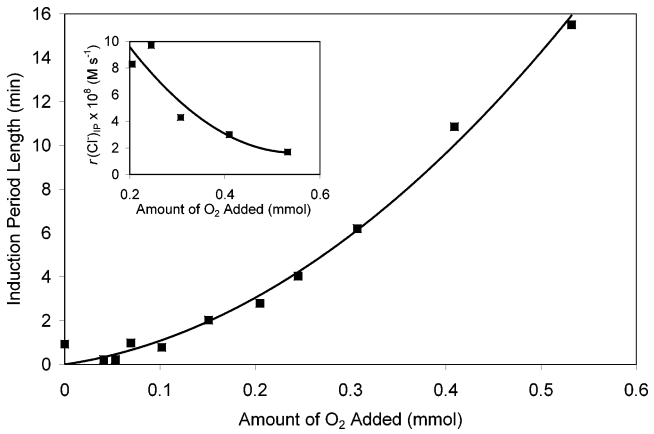

Figure 4. Length of average induction period vs amount of added O_2 for suspensions that were initially degassed with Ar. All suspensions contained 0.30 M formate/formic acid buffer at pH 5.9, 0.50 g L^{-1} TiO_2, and 2.0 mL CFC 11 and were irradiated with $I_o = 1.0 \times 10^{-6}$ M photons s^{-1}. The inset shows the effect of O_2 on $r(Cl^-)$ measured during the first 3 min of the induction period.

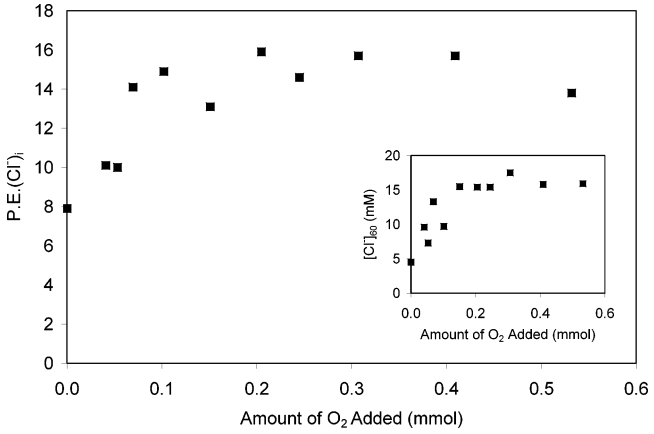

Figure 5. Effect of the amount of added O_2 on P.E.$(Cl^-)_i$ for degassed suspensions with 0.50 g L^{-1} TiO_2, 2.0 mL CFC 11, and 0.30 M formic acid/formate buffer at pH 5.9 and $I_o = 1.0 \times 10^{-6}$ M photons s^{-1}. Shown in the inset are the $[Cl^-]$ obtained after 60 min illumination as a function of the amount of added O_2.

and 5, the initial photonic efficiency increased from 2.8 to 16. Reactions in suspensions at pH > 8 could not be monitored because of the interference of hydroxide ions with the ISE measurements. Chloride ion formation versus time data for reactions at pH 3.0, 4.0, 5.9, and 8.0 displayed in the inset show that the Cl^- yield during the reaction changed with pH in the same manner as P.E.$(Cl^-)_i$. Photoreductions of CCl_3F in suspensions with different pH values exhibited similar induction periods and were identical in all respects, excluding $r(Cl^-)$.

Several experiments were performed using lower light intensities. P.E.$(Cl^-)_i$ increased from 16 to 52 by decreasing I_o from 1.1×10^{-6} to 3.0×10^{-7} M photons s^{-1}. The Cl^- formations were slower at lower light intensities but the decline in $r(Cl^-)_i$ was not as significant as the decrease in I_o. Hence, P.E.$(Cl^-)_i$ increased as the light intensity decreased. However, systematic studies of the dependence of $r(Cl^-)$ on I_o were not possible since low light intensities decreased significantly the rate of chloride production during the induction period. This, in turn, resulted in a very long and less reproducible induction period, which continued for more than 60 min at the lowest light intensity employed.

Figures 4 and 5 depict kinetic aspects of the photoreaction as a function of the amount of O_2 in titania suspensions. Known volumes of O_2 gas were injected into deaerated suspensions prior to irradiation. Figure 4 shows that the average value of the induction period lengthened with the amount of oxygen gas added. Short induction periods, up to 3 min, were measured for air-free systems (average length = 1 min) and were attributed to air leaks that occurred during the injection of liquid CCl_3F.[8] Irradiation of suspensions containing up to 2×10^{-4} moles of O_2 resulted in induction periods indistinguishable from those of analogous air-free suspensions. Addition of 5.3×10^{-4} mol O_2 to a deaerated reaction vessel caused the induction period to last 15 ± 3 min, which was the typical length for air-saturated suspensions. Such a result was expected since that amount of oxygen is within the range of O_2 concentrations estimated for air-saturated suspensions ($5.2-5.5 \times 10^{-4}$ mol).

The inset of Figure 4 illustrates that $r(Cl^-)_{IP}$, the rate of chloride production measured during the first 3 min of the induction period, decreased as the amount of O_2 increased. Data from experiments using less than 2×10^{-4} mol O_2 were not included in the inset since their induction periods were less than 3 min. Although suspensions that initially contained more O_2 exhibited lower rates of chloride formation prior to the onset of the second stage of the reaction, their induction periods were longer. This resulted in higher chloride concentrations measured at the end of the induction period. For instance, chloride yields measured immediately prior to the second step of the reaction steadily increased from 5.8×10^{-5} M to 4.6×10^{-4} M (6.5×10^{-6} to 5.2×10^{-5} moles) as the amount of O_2 increased from 4.1×10^{-5} to 5.3×10^{-4} moles.

Varying the oxygen content of the suspension also affected P.E.$(Cl^-)_i$ and $[Cl^-]_{60}$ ($[Cl^-]$ measured after 60 min of illumination), which was employed to compare Cl^- yields obtained after extended periods of illumination. As portrayed in Figure 5 and in the inset, both quantities increased rapidly with the injection of small amounts of O_2 prior to irradiation until maximum values were achieved at $\sim 1 \times 10^{-4}$ mol O_2. Higher O_2 concentrations had no effect on either the photonic efficiency or the amount of chloride produced. As was the case for the length of the induction period, results of experiments using 5.3×10^{-4} mol O_2 were similar to those of an air-saturated suspension: P.E.$(Cl^-)_i = 14$ and $[Cl^-]_{60} = 16$ mM. Suspensions containing less than 5×10^{-5} moles of O_2 yielded photonic efficiencies and chloride concentrations that approached the corresponding values measured in air-free suspensions.[8]

Experiments were also performed to determine the effects that resulted when O_2 was introduced into air-free suspensions

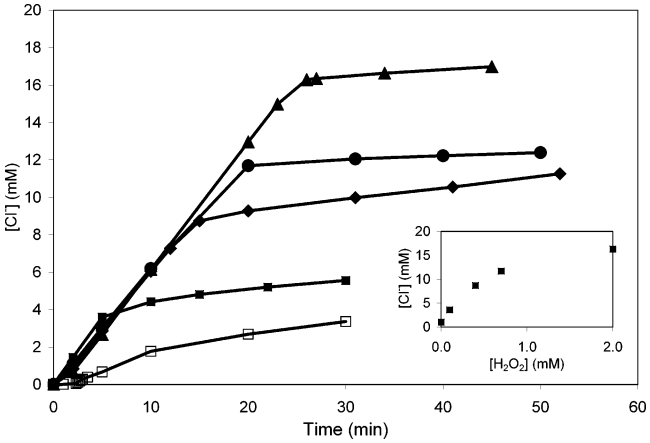

Figure 6. Plot of Cl^- production as a function of time for Ar-saturated suspensions containing zero (□), 0.1 mM (■), 0.4 mM (◆), 0.7 mM (●), and 2.0 mM (▲) H_2O_2. Suspensions were irradiated with $I_o = 1.0 \times 10^{-6}$ M photons s^{-1} and contained 2.0 mL CFC 11, 0.50 g L^{-1} TiO_2, and 0.30 M formic acid/formate buffer at pH 5.9. The inset shows the concentration of Cl^- following the completion of the "fast step" in air-free suspensions as a function of the concentration of H_2O_2 added prior to irradiation.

after the induction period was completed. First, a standard Ar-saturated suspension was prepared and irradiated. After 40 s of irradiation, the maximum reaction rate was measured and then one of the rubber septa used to seal the photoreactor was punctured briefly with a syringe needle. Interestingly, the photoreaction was not quenched by the small amount of air introduced into the vessel. Instead, addition of O_2 increased $r(Cl^-)$ during the rest of the photoreaction since the chloride yield measured after 1 h of irradiation was 7.6 mM. This is 50% higher than $[Cl^-]$ measured in an air-free reaction (5.0 mM) but is much less than the concentration produced in an air-saturated suspension (15 mM). These results agree with the data displayed in Figures 4 and 5, which show that the presence of a small amount of oxygen in the system increased significantly both $r(Cl^-)$ and the yield of chloride ions measured after longer illumination times without lengthening appreciably the induction period.

Earlier studies have shown that photolysis of TiO_2 suspensions containing organic materials and air induces reduction of O_2, forming intermediate peroxide species such as H_2O_2.[11,26−28] Thus, a possible explanation for the enhanced CFC 11 photoreduction when air is introduced in the titania suspensions involves participation of a peroxide in the reduction mechanism. Attempts were made to detect peroxides after the induction period of photolyzed suspensions initially containing air using the iodide method.[28] However, the results were erratic probably because of problems associated with the length of the induction periods and due to the post-irradiation reaction that occurs in the CFC 11 system.[8] Another approach consisted of adding hydrogen peroxide prior to irradiation of air-free suspensions. Figure 6 shows the evolution of $[Cl^-]$ during irradiation of TiO_2 suspensions containing up to 2.0 mM H_2O_2. In all cases, a short induction period was observed, typical of reactions in Ar-saturated systems. After the induction period, Cl^- was generated at its highest rate for a much longer period of time as compared to air-free and air-saturated suspensions. Each of the kinetic runs with peroxide was followed by a blank experiment in which the TiO_2 material was substituted with light-insensitive SiO_2 particles as described in the Experimental Methods section. Insignificant $[Cl^-]$ were detected after extensive illumination, confirming that the data included in Figure 6 resulted from processes initiated by the titania particles and not by direct excitation of H_2O_2.

In the TiO_2 suspensions containing H_2O_2, $r(Cl^-)_i$ remained constant for up to 25 min; the duration of a constant rate of chloride release depended on the amount of H_2O_2 added. In contrast, rapid chloride formation lasted only for 30−40 s for degassed systems and for 1 min in air-saturated suspensions. Following the extended period of rapid chloride production in the H_2O_2 systems, $r(Cl^-)$ suddenly decreased by an order of magnitude or more. Such an abrupt change in reaction rate was also unique to the H_2O_2 systems since chloride formation decreased gradually during extended illumination of suspensions (with or without air) in the absence of added H_2O_2. Although higher $[H_2O_2]$ led to a greater chloride yield, the inset of Figure 6 reveals that $[Cl^-]$ measured at the end of the extended "fast step" began to approach a maximum value of ∼20 mM at high $[H_2O_2]$. Suspensions containing peroxide yielded a $P.E.(Cl^-)_i$ value of 12 irrespective of $[H_2O_2]$, which lies between $P.E.(Cl^-)_i = 7.9$ for air-free suspensions and $P.E.(Cl^-)_i = 16$ for air-saturated systems. On the other hand, $P.E.(F^-)$ measured in an air-free suspension containing 2.0 mM H_2O_2 was 0.58, which is greater than the efficiencies for both an Ar-saturated suspension (0.18) and an air-saturated suspension (0.29).

Discussion

As in the case of the CFC 11 photoreduction in air-free systems,[8] irradiation of TiO_2 suspensions containing trichlorofluoromethane, formate buffer, and O_2 yielded $CHCl_2F$, Cl^-, and small amounts of F^- in a two-stage process. Furthermore, photolysis of suspensions with and without O_2 produced Cl^- concentrations during the second stage that were higher than both the TiO_2 concentration and the solubility limit of CCl_3F in water. These observations mean that in both systems the titania particles acted as sensitizers and that CFC molecules present in the dispersed CCl_3F droplets participated in the photoreactions. Other common features of the CCl_3F phototransformation in suspensions with and without O_2 are (a) small Cl^- and F^- concentrations formed during the induction period (Figure 1 and inset) with a low $[Cl^-]$ to $[F^-]$ ratio (∼3:1); (b) much larger Cl^- and F^- concentrations were photogenerated after the induction period; (c) maximum $r(Cl^-)$ and $r(F^-)$ values were achieved at the beginning of the second step, but the rates declined as the reaction proceeded (Figure 1, Figure 3 inset); (d) significantly more Cl^- than F^- was produced during the second step of the reaction (Figure 1); (e) higher concentrations of formate ions increased the rate of Cl^- generation (Figure 2); (f) low $P.E.(Cl^-)_i$ values were obtained in acidic suspensions (Figure 3); and (g) photonic efficiencies increased as the light intensity decreased.

The fact that $[Cl^-] \gg 3[F^-]$ during the second step confirmed the notion that the photoreaction involved a reduction of CCl_3F to $CHCl_2F$, and not a transformation similar to reaction 1. In analogy to the data obtained with degassed suspensions,[8] the $P.E.(Cl^-)_i$ values shown in Figures 2, 3, and 5 indicate that the rate of product formation was many times greater than the incident light intensity. Efficiencies of product formation much higher than the intensity of incident radiation and inhibition by oxygen are typical features exhibited by free-radical chain reductions of halogenated hydrocarbons, including the CCl_3F photoreduction in TiO_2 systems free of O_2.[6,8−10] Obviously, CFC 11 was photoreduced via a similar free-radical chain process in suspensions initially containing oxygen.

The numerous similarities of the CCl_3F photoreduction in suspensions with and without O_2 mentioned above suggest that

both transformations take place in a somewhat similar manner. The following mechanism was proposed for the photoinitiated chain reduction of CCl_3F in deaerated TiO_2 suspensions:[8]

$$TiO_2 + h\nu \rightarrow h_{vb}^{+} + e_{cb}^{-} \quad (2)$$

$$h_{vb}^{+} + e_{cb}^{-} \rightarrow \text{heat} \quad (3)$$

$$h_{vb}^{+} + H_2O \rightarrow OH^{\bullet} + H^{+} \quad (4)$$

$$h_{vb}^{+}/OH^{\bullet} + HCO_2^{-} \rightarrow {}^{\bullet}CO_2^{-} + H^{+}/H_2O \quad (5)$$

$${}^{\bullet}CO_2^{-} + TiO_2 \rightarrow e_{cb}^{-} + CO_2 \quad (6)$$

$$e_{cb}^{-} + CCl_3F \rightarrow {}^{\bullet}CCl_2F + Cl^{-} \quad (7)$$

$${}^{\bullet}CO_2^{-} + CCl_3F \rightarrow {}^{\bullet}CCl_2F + Cl^{-} + CO_2 \quad (8)$$

$${}^{\bullet}CCl_2F + HCO_2^{-} \rightarrow {}^{\bullet}CO_2^{-} + HCCl_2F \quad (9)$$

$${}^{\bullet}CCl_2F + {}^{\bullet}CO_2^{-} \rightarrow :CClF + Cl^{-} + CO_2 \quad (10)$$

$${}^{\bullet}CCl_2F + e_{cb}^{-} \rightarrow :CClF + Cl^{-} \quad (11)$$

$$:CClF + 2H_2O \rightarrow HCO_2^{-} + 3H^{+} + Cl^{-} + F^{-} \quad (12)$$

Subsequent electron paramagnetic resonance (EPR) measurements have confirmed that ${}^{\bullet}CO_2^{-}$ radicals are photogenerated in degassed TiO_2 suspensions containing formate ions,[12] providing support for the sequence of steps 2−5. The standard reduction potential of conduction band electrons is −0.45 V in the pH 5.9 suspension,[29] and formyl radical anions are stronger reducing agents ($E° = -1.8$ V for $CO_2/{}^{\bullet}CO_2^{-}$).[30] Both ${}^{\bullet}CO_2^{-}$ and e^{-}_{cb} are capable of reducing CCl_3F since $E° = -0.44$ V for the $CCl_3F/{}^{\bullet}CCl_2F$, Cl^{-} redox couple.[31] The kinetics of the CFC photoreduction in air-free suspensions was well rationalized with the mechanism presented above using the following assumptions: (a) steps 7 and 8 contributed equally to start the reduction of CCl_3F, but the latter reaction predominated at longer times; (b) although chain initiation occurred on the oxide surface, propagation steps 8 and 9, as well as the termination sequence of steps 10 and 12, took place mainly in the solution bulk or on the double layer around the oxide particles; (c) step 11 was a minor contributor to chain termination; and (d) adsorption of ${}^{\bullet}CCl_2F$ and :CClF onto the semiconductor surface was insignificant.

Several results of the present study are consistent with these assumptions. For instance, the data of Figure 3 indicate that the CFC reduction remained equally efficient in suspensions with pH values above and below the point of zero charge of 6.2 for P-25 TiO_2.[32,33] Thus, chain propagation was unaffected by the differences in TiO_2 surface chemistry that arise upon changing the pH from 5 to 8. Given the charged nature of ${}^{\bullet}CO_2^{-}$, such observation suggests that chain propagation occurs away from the oxide surface and supports assumption (b). Also, the solubility of CCl_3F in water is unaffected by the TiO_2 particles, which supports assumption (d) because adsorption of the CFC on the oxide surface is negligible. The mechanism above is able to rationalize numerous observations made during the second phase of the reaction in this study. In agreement with step 9, GC-MS measurements detected only $CHCl_2F$ after photolysis of standard suspensions. Dimerizations of ${}^{\bullet}CCl_2F$ and :CClF must not be important termination events because the products of such reactions (FCl_2C-CCl_2F and $FClC=CClF$) were not observed. The high $[HCO_2^{-}]$ present in standard suspensions ensured that hydrogen atom abstraction by ${}^{\bullet}CCl_2F$ was faster than chain termination reactions. As illustrated in Figure 2, lowering $[HCO_2^{-}]$ decreases the photoreaction efficiency since step 9 becomes slower under such conditions, increasing the importance of terminations. Efficient chain propagation via steps 8 and 9 explains the fact that $P.E.(Cl^{-})_i \gg 1$ and also that $[Cl^{-}]/[F^{-}] = 75$ throughout the illumination instead of the 3/1 value anticipated if termination was predominant.

As shown in Figures 1 and 4, O_2 molecules present in the suspensions delayed the onset of the CCl_3F chain photoreaction and decreased $r(Cl^{-})$ during the induction period. A simple interpretation is that oxygen retarded the CFC reduction via consumption of the photogenerated ${}^{\bullet}CO_2^{-}$ and e_{cb}^{-}. Therefore, the induction period corresponded to the time required to transform O_2 into H_2O_2, after which the CFC 11 reduction was to proceed as in air-free systems. However, continuous photolysis beyond the induction period of suspensions that initially contained air always produced more Cl^{-} and at a higher rate than reactions in degassed suspensions of identical composition. $P.E.(Cl^{-})_i$ doubled from 7.9 to 16 and the average chloride concentration after 60 min increased from 5 mM to 16 mM in air-free and air-saturated suspensions, respectively. In fact, the $P.E.(Cl^{-})_i$ values displayed in Figures 2, 3, and 5 are, at least, a factor of 2 higher than the corresponding efficiencies obtained in the absence of O_2.[8] The surprising enhancement of the photoreduction rate by addition of oxygen is best illustrated in Figure 5, which shows a continuous increase in $P.E.(Cl^{-})_i$ with rising amounts of O_2. Larger yields of chloride ions and higher $r(Cl^{-})$ were observed also when a small amount of air was allowed to enter degassed suspensions in which the chain process was already underway.

Obviously, rationalization of the rate enhancements induced by O_2 requires modification of the mechanism described by steps 2−12. Reduction of oxygen via photolysis of TiO_2 electrodes and films in HCO_2H/HCO_2^{-} solutions is known to form peroxides, and some of these remain bound to the oxide surface.[11,26b] This process can be represented by the overall reaction

$$e_{cb}^{-} + {}^{\bullet}CO_2^{-} + O_2 + 2H^{+} \rightarrow H_2O_2 + CO_2 \quad (13)$$

where H_2O_2 is here used to represent both peroxide molecules that remain surface-bound and those that desorb into solution. Reduction of O_2 by e_{cb}^{-} and ${}^{\bullet}CO_2^{-}$ is anticipated to be mainly a surface reaction which is the origin of the induction period. At high $[O_2]$, this process predominates over steps 7 and 8 as well as over the reduction of the peroxide to water. Formation of peroxides on or next to the oxide surface facilitates their reduction via

$$e_{cb}^{-} + H_2O_2 \rightarrow OH^{-} + OH^{\bullet} \quad (14)$$

An analogous reduction of the peroxide by ${}^{\bullet}CO_2^{-}$ occurs;[18] the consequences of such a step will be discussed below. At the high $[HCO_2^{-}]$ present in the suspensions, reaction 14 is followed by a fast step 5, which converts the weakly reducing e_{cb}^{-} into the strong reductant ${}^{\bullet}CO_2^{-}$. In addition to accelerating the reduction of CCl_3F, such conversion hinders charge-carrier recombination (step 2) involving either e_{cb}^{-} or electrons trapped in lattice defects.[4a] An additional advantage of transforming e_{cb}^{-} into ${}^{\bullet}CO_2^{-}$ is that formyl radical anions can diffuse away from the oxide surface, allowing them to react with CCl_3F molecules present in solution and decreasing electron injection via step 6.

Step 14 is predicted to be an important process immediately at the end of the induction period, where the peroxide concentration is highest. The net effect of this process is to increase the number of CCl_3F molecules that are reduced by the photogenerated reductants, leading to higher P.E.$(Cl^-)_i$ values for suspensions that initially contained O_2. Conversion of e^-_{cb} into $^\bullet CO_2^-$ explains why the P.E.$(Cl^-)_i$ values obtained at pH < 5 (see Figure 3) are at least 5 times higher than those determined within the same acidity range for air-free suspensions (Figure 4 of ref 8). In this range of proton concentrations, the reducing power of e_{cb}^- drops increasingly as pH decreases,[8] whereas the redox potential of the $CO_2/^\bullet CO_2^-$ couple remains unchanged (the pK_a of the $^\bullet CO_2H$ radical is 1.4).[31] Although some hydroxyl radicals will react with formic acid at low pH, the resulting $^\bullet CO_2H$ will dissociate to form $^\bullet CO_2^-$ which can then participate in the chain propagation.

Efforts were made to assess numerically the impact of steps 13 and 14 by means of kinetic expressions derived for the oxygen-free system from the standard steady-state approximation for long-chain processes.[8] This derivation was based on the following assumptions: (1) initiation is rate-determining and occurs with a rate equal to that of termination and (2) all propagation steps occur with the same rates, which are much higher than that of the termination process.[16] The effectiveness of chain initiation is represented by ζ_i (the initiation rate (r_{init}) divided by I_o) which measures the fraction of initially photogenerated reductants (e_{cb}^- plus $^\bullet CO_2^-$) that react with CCl_3F. Step 12 is the only source for F^-, and under steady-state conditions, the rate of this reaction is equal to the rate of termination (r_t) and also to r_{init}. Hence, $r(F^-)_i = r_t = r_{init}$, meaning that ζ_i = P.E.$(F^-)_i$ because P.E.$(F^-)_i = r(F^-)_i/I_o$. Occurrence of steps 13 and 14 in suspensions initially saturated with air implies that ζ_i for such systems must be higher than the value measured in the absence of air. Such a prediction is consistent with the data since P.E.$(F^-)_i = 0.29$ for air-saturated suspensions whereas a value of 0.18 was typical of air-free systems.

The P.E.$(F^-)_i$ value also enables estimation of the kinetic chain length (kcl) that is available from the ratio r_p/r_t = P.E.$(Cl^-)_i$/P.E.$(F^-)_i$, where r_p is the propagation rate. For air-saturated suspensions, kcl = 55, as compared with a value of 44 determined for air-free systems. Such large kcl values justify the use of the steady-state approximation. Another consequence of this approximation is that the cross-termination step 10 involving both chain carriers, $^\bullet CO_2^-$ and $^\bullet CCl_2F$, is only feasible if their steady-state concentrations are very similar, $[^\bullet CO_2^-]_{ss} \approx [^\bullet CCl_2F]_{ss}$. Evaluation of these concentrations was possible from eqs 13 and 17 of ref 8, together with the kinetic parameters obtained for air-free systems and the ζ_i value of air-saturated suspensions. The results were $[^\bullet CO_2^-]_{ss} = 1.8 \times 10^{-8}$ M and $[^\bullet CCl_2F]_{ss} = 1.0 \times 10^{-8}$ M as compared with 1.4×10^{-8} M and 1.2×10^{-8} M, respectively, for analogous air-free systems.[8] Evaluation of k_8 and k_9 (by means of eqs 15 and 16, ref 8) yielded 1.1×10^5 and 3.1×10^3 M^{-1} s^{-1}, respectively, which compare well with the earlier values of 7.2×10^4 and 1.9×10^3 M^{-1} s^{-1}.

Despite the reasonable agreement between the concentrations of chain carriers and of the rate constants from the present and previous studies, other results were not entirely consistent with the mechanism. An example is the test carried out by means of the rate law derived for the photoreduction of CCl_3F in suspensions free of O_2[8]

$$r(Cl^-)_i = (k_8\, k_9\, \zeta_i\, I_o/k_{10})^{0.5}([HCO_2^-][CCl_3F])^{0.5} \quad (15)$$

which was obtained from the rate equation of step 8 and the standard steady-state approximations for long-chain processes. In this expression, k_8, k_9, and k_{10} are the rate constants of the corresponding elementary steps in the mechanism. Data from the inset of Figure 2 is consistent with the relationship between $r(Cl^-)_i$ and $[HCO_2^-]^{0.5}$ predicted by eq 15. Confirmation of the dependence of $r(Cl^-)_i$ on $I_o^{0.5}$ was not feasible because of the experimental difficulties mentioned before but a few runs carried out at low light intensity yielded lower reaction rates, providing qualitative support for the rate law. As in the air-free system,[8] verification of the dependence of $r(Cl^-)_i$ on $[CCl_3F]^{0.5}$ was impossible because of the limited solubility of the CFC in H_2O. Tests of the validity of eq 15 in systems containing O_2 consisted of finding the ζ_i value required to obtain P.E.$(Cl^-)_i = 16$, the typical value for air-saturated systems, using $k_8 = 7.2 \times 10^4$ M^{-1} s^{-1}, $k_9 = 1.9 \times 10^3$ M^{-1} s^{-1}, $k_{10} = 1 \times 10^9$ M^{-1} s^{-1}, $I_o = 1.1 \times 10^{-6}$ M photons s^{-1}, $[HCO_2^-] = 0.30$ M, and $[CCl_3F] = 8.1 \times 10^{-3}$ M. The calculation yielded $\zeta_i = 0.85$ instead of the experimental value of 0.29.

This discrepancy implies that the mechanistic sequence of steps 2−14 is unable to describe well the effect exerted by O_2 and that additional processes must be taken into consideration. Oxygen reacts fast with halogenated carbon-centered radicals,[23b,34] for example, $^\bullet CCl_3$ forms $^\bullet O_2CCl_3$ with $k = 2-3 \times 10^9$ M^{-1} s^{-1}. Generation of $^\bullet O_2CCl_2F$ is known to occur via[34b]

$$O_2 + {}^\bullet CCl_2F \rightarrow {}^\bullet O_2CCl_2F \quad (16)$$

k_{16} has not been determined but should be similar to that for the analogous reaction involving $^\bullet CCl_3$. Halogenated peroxy radicals are oxidizers and $^\bullet O_2CCl_3$ abstracts a H atom from 2-propanol with $k = 7 \times 10^3$ M^{-1} s^{-1}.[35] Hence, the following reaction seems reasonable because HCO_2^- and 2-propanol exhibit similar abilities as H-donors

$$^\bullet O_2CCl_2F + HCO_2^- \rightarrow {}^\bullet CO_2^- + HO_2CCl_2F \quad (17)$$

Halogenated hydroperoxides decay in water with complete loss of all halogen atoms via a mechanism that remains unclear;[36] an analogous reaction seems feasible for HO_2CCl_2F

$$HO_2CCl_2F + H_2O \rightarrow 2Cl^- + F^- + \text{products} \quad (18)$$

The sequence of steps 16−18 is one of the possible mechanisms that can contribute to the complete decay of CCl_3F during the induction period according to the overall reaction 1. However, occurrence of step 16 is questionable after the induction period in view of the low $[O_2]$ that remains in the aqueous phase. On the other hand, numerous small CCl_3F droplets are present in the stirred suspensions, and surrounding each of them is a thin layer called the diffusion film.[37] In this region, $[CCl_3F]$ decreases continuously from 10.9 M (the molarity of pure CCl_3F at the droplet surface) to the limiting solubility in water. Both $[HCO_2^-]$ and $[^\bullet CO_2^-]$ are lower in this region than in the aqueous phase. These facts together with the higher oxygen solubility in the CFC than in H_2O imply that $[O_2]$ is larger in the diffusion film than in the aqueous electrolyte. This means that the phase-segregated CFC dispersed in the aqueous electrolyte is the most probable place for reaction 16 to take place. Although the hydrolytic step 18 produces F^-, the combination of such a reaction with steps 16 and 17 is not a chain termination process because $^\bullet CO_2^-$ is regenerated. In other words, incorporation of steps 16−18 into the sequence of reactions 2−14 results in a more complex mechanism, which will exhibit a rate law different from eq 15 because $r(F^-)$ no longer measures the rate of termination.

The data presented in Figure 6 provides some support to the idea that in suspensions initially containing O_2, peroxides produced during the induction period aided the subsequent photoreduction of CCl_3F. Introduction of H_2O_2 into degassed suspensions prior to irradiation circumvented the loss of e_{cb}^- and $^\bullet CO_2^-$ via step 13 and increased P.E.$(Cl^-)_i$ without lengthening the induction period. Although the disproportionation of H_2O_2 generates O_2, this reaction is very slow at room temperature even in the presence of suspended titania particles.[38] Hence, addition of peroxide to the suspensions resulted in O_2 amounts too low to affect the length of the induction periods. H_2O_2 adsorbs on TiO_2 surfaces when peroxide solutions are in contact with titania.[11,39] Rough estimates of the peroxide adsorption onto the particles were obtained using reported values[39b] and yielded quantities amounting to about 2% of the H_2O_2 added to the suspensions. These estimates are useful to interpret the data displayed in Figure 6, which yielded a P.E.$(Cl^-)_i$ value (12) that is 50% higher than in the absence of peroxide and is independent of $[H_2O_2]$. Such results imply that enough H_2O_2 was adsorbed in all cases to efficiently convert e_{cb}^- into $^\bullet CO_2^-$ through steps 14 and 5. According to this interpretation, the photoreduction of CCl_3F in the presence of H_2O_2 proceeds via steps 2−12 together with step 14, where the main change is a ζ_i value higher than the initiation efficiency found without peroxide.

Several observations support this simple mechanism, including the fact that ζ_i = P.E.$(F^-) = 0.58$ for suspensions containing 2.0 mM H_2O_2 whereas an efficiency of 0.18 was determined without peroxide. Also, a ζ_i value of 0.48 was needed to obtain P.E.$(Cl^-)_i = 12$ via eq 15; such an efficiency agrees well with the experimental result. Another feature typical of suspensions containing H_2O_2 shown in Figure 6 is that $[Cl^-]$ increased linearly with time for periods much longer than in degassed systems without peroxide.[8] Addition of larger amounts of H_2O_2 extended the length of time during which the system yielded a P.E.$(Cl^-)_i$ of 12, up to 25 min when $[H_2O_2] = 2.0$ mM. Consequently, longer initial periods of maximum chloride formation were due to the continuous transformation of H_2O_2 into $^\bullet CO_2^-$ radicals. Such a transformation occurred efficiently because any surface-bound peroxide consumed during the photoreaction was promptly replaced through adsorption from solution.

Interestingly, kcl was 20.7 for the suspensions with 2.0 mM H_2O_2, indicating that the photoreaction proceeded with an average chain length at least 2 times shorter than those of systems without peroxide. Occurrence of shorter chains in the peroxide systems can be understood in terms of reaction 19

$$H_2O_2 + {}^\bullet CO_2^- \rightarrow OH^- + OH^\bullet + CO_2 \qquad (19)$$

which in solution takes place with $k_{19} = 6 \times 10^5\ M^{-1}\ s^{-1}$.[40] Although any $^\bullet CO_2^-$ radical consumed through this process will be regenerated via reaction 5, step 19 competes with step 8 and retards chain propagation. Further evidence that the retardation reaction limits the extent of the CFC photoreduction is obtained upon analysis of the data shown in the inset of Figure 6. The final Cl^- concentration photogenerated during the fast stage was a nonlinear function of the peroxide concentration, and the ratio of the final $[Cl^-]$ to $[H_2O_2]$ decreased continuously from 36 to 8 upon increasing the peroxide concentration from 0.1 to 2 mM. A similar trend is obtained from r_8/r_{19} (the ratio of rates from steps 8 and 19), which decreased continuously from 9.7 to 0.49 over the same range of $[H_2O_2]$ values. Obviously, chain retardation via step 19 turns increasingly important at higher peroxide concentrations. In the simple mechanism, the propagation steps occurred mainly in the solution bulk, implying that consumption of peroxide molecules present in the liquid phase via step 19 limits their adsorption on the oxide surface.

Hydrogen peroxide has been found to increase the rate of photooxidation induced by TiO_2 suspensions of several environmental pollutants, including phenol,[41] pesticides,[42] chlorinated organic compounds,[43] and *Escherichia coli*.[44] A declining influence of H_2O_2 at high concentrations has been noted in several of these studies, and the optimal concentration of H_2O_2 was also determined to be in the millimolar range. Although the effects induced by H_2O_2 on the photoreduction of CCl_3F have been rationalized exclusively in terms of steps 14 and 19, recent results suggest that adsorption of the peroxide on the TiO_2 surface yields a complex that is photosensitive.[45] The photodegradation of such complex may contribute to the limiting effect of the peroxide action in suspensions containing high $[H_2O_2]$.

Conclusion

Irradiation of air-saturated titanium dioxide suspensions containing HCO_2^- and CCl_3F with UV light yields Cl^- and $CHCl_2F$ through a free-radical chain reaction. Consumption of O_2 during the induction period generates an increased number of $^\bullet CO_2^-$ radicals that can initiate the chain process. Reaction steps that occur in addition to those proposed for analogous reactions in deaerated suspensions are consistent with the experimental kinetic data showing higher P.E.$(Cl^-)_i$ following a longer induction period.

Acknowledgment. This paper is dedicated to Professor M. R. Hoffman on his 60th birthday. We thank Degussa for the donation of TiO_2 and SiO_2 powder samples. We are grateful to Drs. G. Goodloe and E. Hughes for performing the GC-MS measurements. The Florida Solar Energy Center and NTC/DOC partially funded this research; the U.S. Navy CIVINS program supported the work of R.L.C.

References and Notes

(1) (a) Rao, T. N.; Tryk, D. A.; Fujishima, A. In *Encyclopedia of Electrochemistry*; Bard, A. J., Stratmann, M., Eds.; Wiley: New York, 2002; Vol. 6, p 536. (b) Kisch, H. *Advances in Photochemistry*; Neckers, D. C., von Bunau, G., Jenks, W. S., Eds.; John Wiley: New York, 2001; p 93.

(2) Mills, A.; Le, Hunte, G. *J Photochem. Photobiol., A* **1997**, *108*, 1.

(3) Hoffmann, M. R.; Martin, S. T.; Choi, W.; Bahnemann, D. W. *Chem. Rev.* **1995**, *95*, 69.

(4) (a) Rajh, T.; Ostafin, A. E.; Micic, O. I.; Tiede, D. M.; Thurnauer, M. C. *J. Phys. Chem.* **1996**, *100*, 4538. (b) Micic, O. I.; Zhang, Y.; Cromak, K. R.; Trifunac, A. D.; Thurnauer, M. C. *J. Phys. Chem.* **1993**, *97*, 7277.

(5) (a) Geshuni, S.; Itzhak, N.; Rabani, J. *Langmuir* **1999**, *15*, 1141. (b) Huang, Z. Y.; Barber, T.; Mills, G.; Morris, M.-B. *J. Phys. Chem.* **1994**, *98*, 12746. (c) Hoffman, A. J.; Yee, H.; Mills, G.; Hoffmann, M. R. *J. Phys. Chem.* **1992**, *96*, 5540. (d) Hoffman, A. J.; Mills, G.; Yee, H.; Hoffmann, M. R. *J. Phys. Chem.* **1992**, *96*, 5546.

(6) Radlowski, C.; Sherman, W. V. *J. Phys. Chem.* **1970**, *74*, 3043.

(7) Shen, T.-L.; Wooldridge, P. J.; Molina, M. J. In *Composition, Chemistry and Climate of the Atmosphere*; Singh, H. B., Ed.; Van Nostraud Reinhold: New York, 1995; Chapter 12.

(8) Calhoun, R. L.; Winkelmann, K.; Mills, G. *J. Phys. Chem. B* **2001**, *105*, 9739.

(9) Weaver, S.; Mills, G. *Phys. Chem. B* **1997**, *101*, 3769.

(10) (a) Stark, J.; Rabani, J. *J. Phys. Chem. B* **1999**, *103*, 8524. (b) Choi, W.; Hoffmann, M. R. *Environ. Sci. Technol.* **1997**, *31*, 89.

(11) Augustynski, J. In *Structure and Bonding. Solid Materials*; Springer-Verlag: Berlin, 1988; Vol. 69, p 1.

(12) Perissinotti, L. L.; Brusa, M. A.; Grela, M. A. *Langmuir* **2001**, *17*, 8422.

(13) Schwarz, H. A.; Dodson, R. W. *J. Phys. Chem.* **1984**, *88*, 3643.

(14) Hu, C.-M.; Tu, M.-H. *J. Fluorine Chem.* **1991**, *55*, 105.

(15) (a) Powell, R. L. *J. Fluorine Chem.* **2002**, *114*, 237. (b) McCulloch, A. *J. Fluorine Chem.* **1999**, *100*, 163. (c) Wallington, T. J.; Schneider, W.

F.; Worsnop, D. R.; Nielsen, O. J.; Sehested, J.; Debruyn, W.; J.; Shorter, J. A. *Environ. Sci. Technol.* **1994**, *28*, 320A.

(16) Huyser, E. S. *Free-Radical Chain Reactions*; Wiley-Interscience: New York, 1970; Chapter 3.

(17) Malone, K.; Weaver, S.; Taylor, D.; Cheng, H.; Sarathy, K. P.; Mills, G. *J. Phys. Chem. B* **2002**, *106*, 7422.

(18) Neta, P.; Huie, R. E.; Ross, A. B. *J. Phys. Chem. Ref. Data* **1988**, *17*, 1027.

(19) Horvath, A. L. *Halogenated Hydrocarbons: Solubility-Miscibility with Water*; Marcel Dekker: New York, 1982; pp 661−710.

(20) *CRC Handbook of Chemistry and Physics*, 73rd ed.; Lide, D. R., Ed.; CRC Press: Boca Raton, FL, 1992; pp 6-3, 6-4, 6-8, and 6-9.

(21) Heller, H. G.; Langan, J. R. *J. Chem Soc., Perkin Trans. 2* **1981**, 341.

(22) Salinaro, A.; Emeline, A. V.; Zhao, J.; Hidaka, H.; Ryabchuk, V. K.; Serpone, N. *Pure Appl. Chem.* **1999**, *71*, 321.

(23) (a) Huston, P. L.; Pignatello, J. J. *Environ. Sci. Technol.* **1996**, *30*, 3457. (b) Mönig, J.; Bahnemann, D.; Asmus, K.-D. *Chem.-Biol. Interact.* **1983**, *45*, 15.

(24) (a) Calza, P.; Minero, C.; Pelizzetti, E. *Environ. Sci. Technol.* **1997**, *31*, 2198. (b) Hilgendorff, M.; Hilgendorff, M.; Bahnemann, D. W. *J. Adv. Oxid. Technol.* **1996**, *1*, 35.

(25) (a) Serpone, N.; Terzian, R.; Minero, C.; Pelizzetti, E. In *Photosensitive Metal-Organic Systems*; Kutal, C., Serpone, N., Eds.; Advances in Chemistry Series 238; American Chemical Society: Washington, DC, 1993; p 281. (b) Cunningham, J.; Al-Sayyed, G.; Srijarani, S. In *Aquatic and Surface Photochemistry*; Helz, G. R., Zepp, R. G., Crosby, D. G., Eds.; CRC Press: Boca Raton, FL, 1994; p 317.

(26) (a) Goto, H.; Hanada, Y.; Ohno, T.; Matsumura, M. *J. Catal.* **2004**, *225*, 223. (b) Shiraishi, F.; Nakasako, T.; Hua, Z. *J. Phys. Chem. A* **2003**, *107*, 11072. (c) Gerischer, H.; Heller, A. *J. Phys. Chem.* **1991**, *95*, 5261.

(27) Ikeda, K.; Sakai, H.; Baba, R.; Hashimoto, K.; Fujishima, A. *J. Phys. Chem. B* **1997**, *101*, 2617.

(28) Mills, G.; Hoffmann, M. R. *Environ. Sci. Technol.* **1993**, *27*, 1681.

(29) Grätzel, M. *Heterogeneous Photochemical Electron Transfer*; CRC Press: Boca Raton, FL, 1988; p 106.

(30) Schwarz, H. A.; Dodson, R. W. *J. Phys. Chem.* **1984**, *88*, 3643.

(31) Stanbury, D. M. *Adv. Inorg. Chem.* **1989**, *33*, 69.

(32) Akratopolu, K. Ch.; Kordulis, C.; Lycourghiotis, A. *J. Chem. Soc., Faraday Trans.* **1990**, *96*, 3437.

(33) (a) Faffrezic-Renault, N.; Pichat, P.; Foissy, A.; Mercier, R. *J. Phys. Chem.* **1986**, *90*, 2733. (b) Jansen, M. J. G.; Stein, H. N. *J. Colloid Interface Sci.* **1986**, *109*, 508.

(34) (a) Lal, M.; Schönich, C.; Mönig, J; Asmus, K.-D. *Int. J. Radiat. Biol.* **1988**, *54*, 773. (b) Alfassi, Z. B.; Mosseri, S.; Neta, P. *J. Phys. Chem.* **1987**, *91*, 3383.

(35) Parker, J. E.; Mahood, J. S.; Wilson, R. L.; Wolfenden, B. S. *Int. J. Radiat. Biol.* **1981**, *39*, 135.

(36) Fliount, R.; Makogon, O.; Asmus, K.-D. *J. Phys. Chem. A* **1997**, *101*, 3547.

(37) Cox, B. G. *Modern Liquid Phase Kinetics*; Oxford University Press: New York, 1994; Chapter 6.

(38) Hiroki, A.; LaVerne, J. A. *J. Phys. Chem. B* **2005**, *109*, 3364.

(39) (a) Jenny, B.; Pichat, P. *Langmuir* **1991**, *7*, 947. (b) Boonstra, A. H.; Mutsaers, C. A. H. A. *J. Phys. Chem.* **1975**, *79*, 1940.

(40) Schwarz, H. A. *J. Phys. Chem.* **1992**, *96*, 8937.

(41) (a) Auguliaro, V.; Davi, E.; Palmisano, L.; Schiavello, M.; Sclafani, A. *Appl. Catal.* **1990**, *65*, 101. (b) Wei, T.-Y.; Wang, Y.-Y.; Wan, C.-C. *J. Photochem. Photobiol., A.* **1990**, *55*, 115.

(42) Doong, R.; Chang, W. *J. Photochem. Photobiol., A* **1997**, *107*, 239.

(43) Dionysiou, D. D.; Suidan, M. T.; Bekou, E.; Baudin, I.; Laine, J.-M. *Appl. Catal. B: Environ.* **2000**, *26*, 153.

(44) Rincon, A.-G.; Pulgarin, C. *Appl. Catal., B* **2004**, *51*, 283.

(45) Li, X.; Chen, C.; Zhao, J. *Langmuir* **2001**, *17*, 4118.